CHAPTER : 9

EFFECT OF PARTIAL REPLACEMENT OF SELENIUM BY SULPHUR ON PHOTOELECTROCHEMICAL BEHAVIOUR OF WSe_2

9.1 INTRODUCTION :

While comparing a liquid junction phtoelectrochemical (PEC) solar cell with conventional solid state p-n junction solar cell it is seen that in the fabrication of PEC devices, many processing steps required for p-n junction solar cells are either simplified or eliminated. Therefore, there is a significant reduction in cost in the fabrication of a PEC device relative to a solid state solar cell. Moreover, PEC devices can also be used to store energy in the form of conventional fuels.

Several layered materials [1] possess favourable semiconducting properties and have attracted attention as a new class of solar cell materials. An attempt to use layered semiconducting tin dichalcogenides in the fabrication of PEC solar cells was made by Katty and his group [2,4], but conversion efficiencies reported by them are very low. Also, in view of a poor photoresponse observed with tin sulphoselenide in this laboratory, author concentrated to look for TMDC having maximum potential for PEC solar cells. For, this purpose, a critical literature survey was made by the author. It was seen that among the layered TMDCs, tungstendichalcogenides (WSe_2 and WS_2) had been extensively studied and used as photoelectrodes in PEC solar cells. Single crystals of n-WSe_2 had shown reasonable conversion efficiency in liquid junction cells - 14% for red light [5] and greater than 13% for solar illumination [6]. Lately values upto 17% [7] and 22% [8] efficiency in energy conversion have been reported for single crystals of n-WSe_2 photoelectrodes. Therefore, research on WSe_2 photoelectrode material takes a step closer to a viable liquid junction (PEC) solar cell. Thus, a lot of research work is being done to study the effect of different parameters for the enhancement of efficiency of PEC solar cells fabricated with WSe_2. In this context, the author has studied the effect of partial replacement of selenium by sulphur

in the lattice of WSe_2 on the photoconversion behaviour of WSe_2 PEC solar cells. The results of this study are described in this chapter.

9.2 EXPERIMENTAL AND OBSERVATIONS :

9.2.1 SELECTION OF MATERIAL :

Single crystals of WSe_2 and WSSe required for the present work were grown by a direct vapour transport method (Chapter 2). Growth conditions pertaining to the growth of these crystals are summarised in Table 9.1. Care has been taken to select the samples from the same batch. All the crystals when characterised by EDAX for their compositional analysis indicated that all of them are nearly stoichiometric. Electrical characterisation of the samples showed that all of them possess p-type semiconducting nature.

9.2.2 SAMPLE PREPARATION :

Step free (vdW) surfaces i.e. crystals with absolutely plane faces were procured after a careful examination of the samples under an Epignost optical microscope. In order to see the effect of partial replacement of selenium by sulphur in the host lattice of WSe_2 on the photoresponse, all the samples of WSe_2 and WSSe were deliberately chosen to be step free. Such surfaces could be easily prepared by the act of cleavage.

9.2.3 ELECTRODE FABRICATION :

A glass rod 0.5 cm in diameter and 10 to 12 cm in length with narrow bore of diameter 0.05 cm was used to prepare the electrode.

Table 9.1 : Growth conditions of WSe_2 and WSSe single crystals using a DVT Technique.

Crystal	Dimensions of the ampoule		Temp. at which the compound was prepared (^0C)	Time for which the ampoule was kept for compound preparation (days)	Temp. range (T_1 - T_2) at which the ampoule was kept in the furnace for growth of single crystals (^0C)	Rate at which the temp. was increased from room temp. to the temp. range T_1 - T_2 (^0C/hr)	Time for which the ampoule was kept in the temp. range (T_1 - T_2) days	Rate at which the ampoule was brought down to room temperature ^0C/hr.	Size of the crystals cm × cm	Thickness of the crystals (μm)
	Internal Diameter cm	Length cm								
WSe_2	2.5	24.0	800	3	950 - 750	50	10	5	1.9 × 1.0	26
WSSe	2.5	24.0	800	3	1010 - 800	50	10	5	1.0 × 0.8	12

One end of this narrow bore glass rod was flattened by hot gas blow. The flat portion was used as a platform for resting the crystal. The narrow bore was used as a passage for traversing a good conducting copper wire. The copper wire was flattened at one end for getting a contact with the crystal.

A semiconductor electrode using single crystals used in the present work was fabricated in such a way that the contacting material (adhesive silver paste) provided good ohmic contact between the copper wire and the back side of the crystal. The whole assembly was then kept in an oven for few hours at 100° C for baking. After proper setting of the crystal on the copper wire terminal, the back side of the semiconductor was covered with an epoxy resin (araldite) leaving a light exposed area of about 2 - 5 mm^2. The so prepared complete device of the electrode is shown in Fig. 9.1.

9.2.4 SOLAR CELL FABRICATION :

The semiconductor electrode prepared in the manner outlined above was immersed in an appropriate electrolyte contained in a corning glass beaker. A platinum grid (3 cm x 3 cm) was used as the counter electrode. A schematic diagram showing the PEC solar cell is given in Fig. 9.2. The cell was illuminated with light from an incandescent lamp. The intensity of illumination was altered by changing the distance between the light source and the electrode. The incident intensity of illumination was measured using 'Suryamapi' the light measuring instrument furnished by Central Electronics Limited, India. Photocurrents and photovoltage were recorded using digital multimeters.

9.2.5 SELECTION OF APPROPRIATE ELECTROLYTE :

The best reported redox electrolyte for n- WSe_2 and p- WSe_2 was

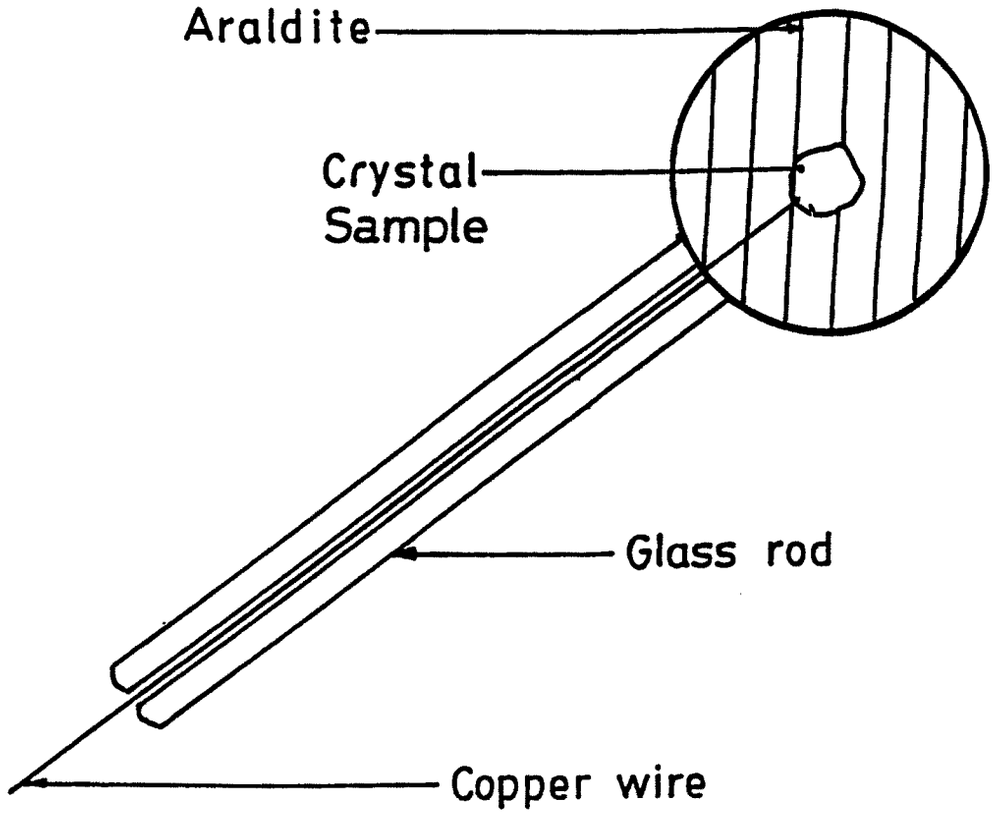

Fig. 9.1 Schematic diagram of photoelectrode.

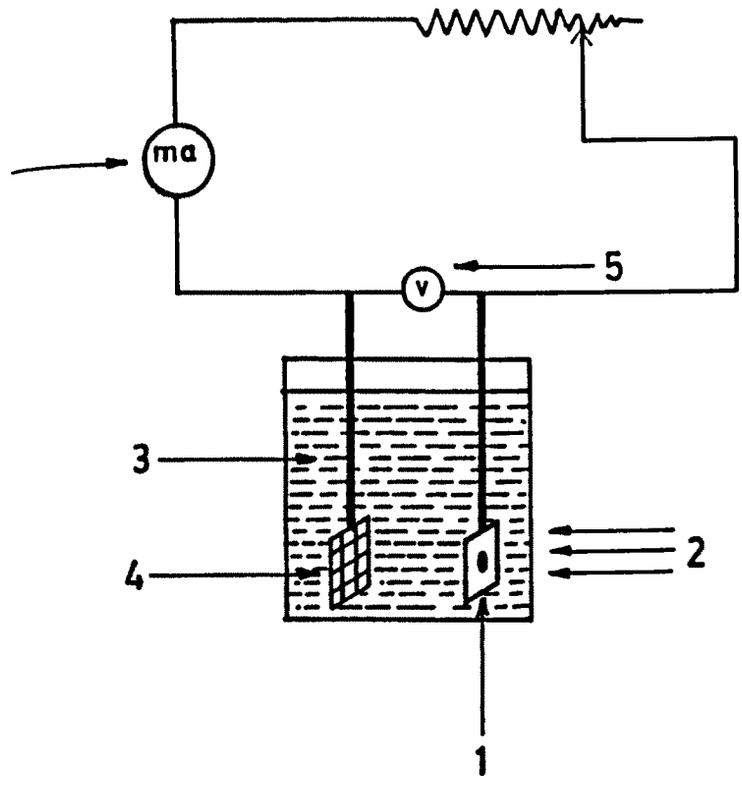

1 Semi conducting crystal.
2 Incident light.
3 Electrolyte
4 Platinum grid
5 Voltmeter
6 Milliammeter

Fig. 9.2 Schematic diagram of PEC solar cell.

an I_2/I^- solution [6 - 16]. A mixture of sodium iodide (Na I), Iodine (I_2), sodium sulphate (Na_2SO_4) and sulphuric acid (H_2SO_4) was employed as an electrolyte. All the chemical products were of reagent grade and the electrolyte solutions were prepared using distilled water. The solutions were not stirred during the measurements.

Thirty different electrolytes with different amounts of reagents were prepared. For determining the suitable electrolyte, photoelectrodes were prepared with WS_xSe_{2-x} (x = 0 and x = 1) single crystals having visibly smooth surfaces as obtained by an act of cleavage with an adhesive tape. The smoothness of the surfaces was ascertained by an Epignost optical microscope (Chapter 2).

Keeping the light intensity of 100 mW/cm^2, dark current I_D, dark voltage V_D, photovoltage (Vp) and photocurrent (Ip) were measured for both (p-WSe_2 and p-WSSe) electrodes in all the electrolytes and it was observed that electrolyte with the composition 1M NaI + 0.025 I_2 + 2M Na_2SO_4 + 0.5M H_2SO_4 gave the minimum dark voltage (V_D = 0.1 mV) and dark current (I_D = 0.1 μM) and as well provided the maximum value of photocurrent and photovoltage for both the electrodes.

The suitability of this electrolyte for the electrodes giving maximum photoresponse was also ascertained from the Mott-Schottky plots described below.

9.2.6 MOTT-SCHOTTKY EVALUATION :

9.2.6.1 Capacitance Measurements :

The capacitance of solid/liquid interface in the PEC solar cells vary

from a few μF to pF. It becomes highly difficult to measure the values accurately using normal laboratory capacitance meters. To measure the space charge capacitance in the above mentioned range. The Hewlett Packard LCR meter (Chapter 2) was deployed. The schematic diagram for impedance measurements is demonstrated in Fig. 9.3. A saturated calomel electrode (SCE) was used as a reference electrode and platinum grid as a counter electrode.

9.2.6.2 Mott-Schottky Plots :

Capacitance measurements shown in Tables 9.2 and 9.3 were undertaken with p-WSe_2 and p-WSSe electrodes at various potentials. Capacitance data from these electrodes were carried out to construct Mott-Schottky plots ($\frac{1}{C_{sc}^2}$ versus V). Figs. 9.4 and 9.5 present such plots for WSe_2 and WSSe single crystal electrodes in the electrolyte (1M NaI + 0.025M I_2 + 2M Na_2SO_4 + 0.5M H_2SO_4). The plots show good straight line behaviour over the potential range employed.

In the graphs of $\frac{1}{C_{sc}^2}$ versus V (Figs. 9.4 and 9.5) the voltage axis intercept gives the flat band potential V_{fb} [Table 9.4] which in the present case are obtained as 0.22 V for WSe_2 and 0.04 V for WSSe. The acceptor concentration N_A for WSe_2 and WSSe crystals can be determined from the slopes of the Mott-Schottky plots in Figs. 9.4 and 9.5 by using the formula

$$N_A = 2[e\,\varepsilon\,\varepsilon_o \times \text{Slope}]^{-1} \qquad (9.1)$$

Where N_A is the acceptor concentration, e is the charge of the electron taken as 1.602×10^{-19} coulomb, ε is the dielectric constant of the material, ε_o is the permittivity with a value of 8.854×10^{-12} Fm^{-1}.

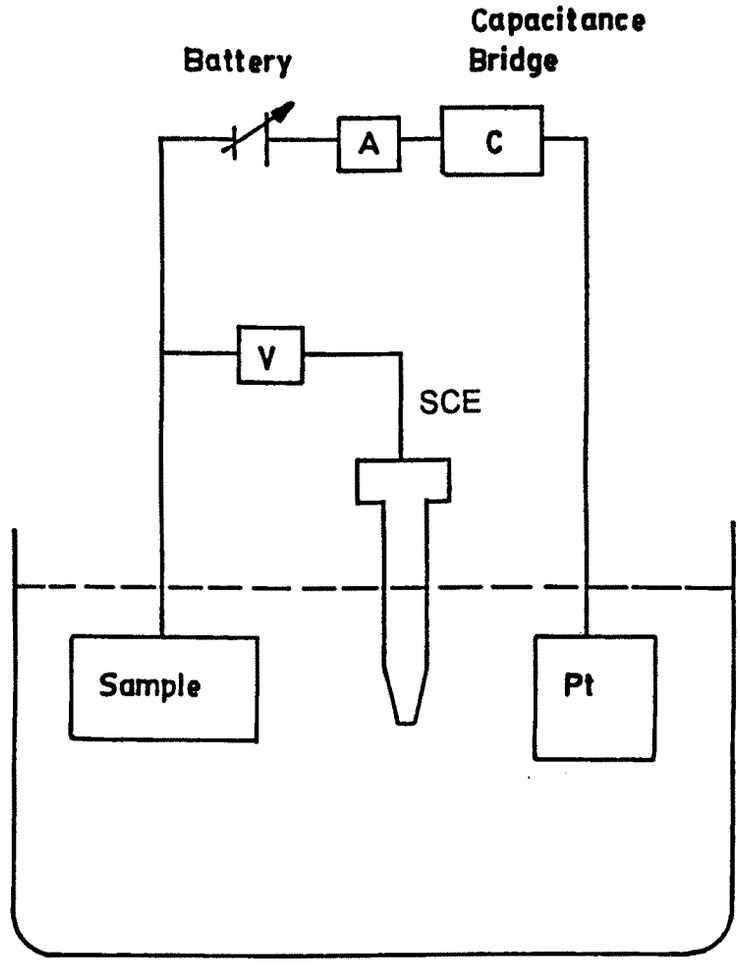

Fig. 9.3 Schematic diagram for impedance measurements.

Table 9.2 : Data from Capacity measurement : Mott Schottky Plot

Crystal : WSe_2

Type : p - type

Input Intensity : 100 mW/cm^2

Electrolyte : 0.025M I_2 + 1M NaI + 2M Na_2SO_4 + 0.5M H_2SO_4

Surface : Plane, obtained after cleaving the as grown face

Contact : Silver paste

Area of the electrode surface : $1.125 \times 10^{-5}\ m^2$

Applied Potential V_{scE}(V)	Capacitance F	C_{sc} C/area F/m^2	$\frac{1}{C_{sc}^2}$ m^4/F^2
-0.7	1.86×10^{-9}	1.66×10^{-4}	3.65×10^{7}
-0.6	1.96×10^{-9}	1.75×10^{-4}	3.28×10^{7}
-0.5	2.06×10^{-9}	1.83×10^{-4}	2.99×10^{7}
-0.4	2.28×10^{-9}	2.02×10^{-4}	2.44×10^{7}
-0.3	2.49×10^{-9}	2.21×10^{-4}	2.05×10^{7}
-0.2	2.60×10^{-9}	2.31×10^{-4}	1.88×10^{7}
-0.1	3.12×10^{-9}	2.77×10^{-4}	1.30×10^{7}
0.0	3.47×10^{-9}	3.08×10^{-4}	1.05×10^{7}

Table 9.3 : Data from Capacity measurement : Mott Schottky Plot

Crystal : WSSe

Type : p - type

Input Intensity : 100 mW/cm^2

Electrolyte : 0.025M I_2 + 1M NaI + 2M Na_2SO_4 + 0.5M H_2SO_4

Surface : Plane obtained after cleaving the as grown face

Contact : Silver paste

Area of the electrode surface : 3.75×10^{-6} m^2

Applied Potential V_{SCE}(V)	Capacitance F	C_{sc} C/area F/m^2	$\frac{1}{C_{sc}^2}$ m^4/F^2
-1.0	4.72×10^{-12}	1.26×10^{-6}	6.31×10^{11}
-0.8	5.27×10^{-12}	1.41×10^{-6}	5.06×10^{11}
-0.6	6.09×10^{-12}	1.62×10^{-6}	3.79×10^{11}
-0.4	7.50×10^{-12}	2.00×10^{-6}	2.50×10^{11}
-0.2	1.01×10^{-11}	2.69×10^{-6}	1.38×10^{11}
0.0	2.53×10^{-11}	6.74×10^{-6}	2.20×10^{10}

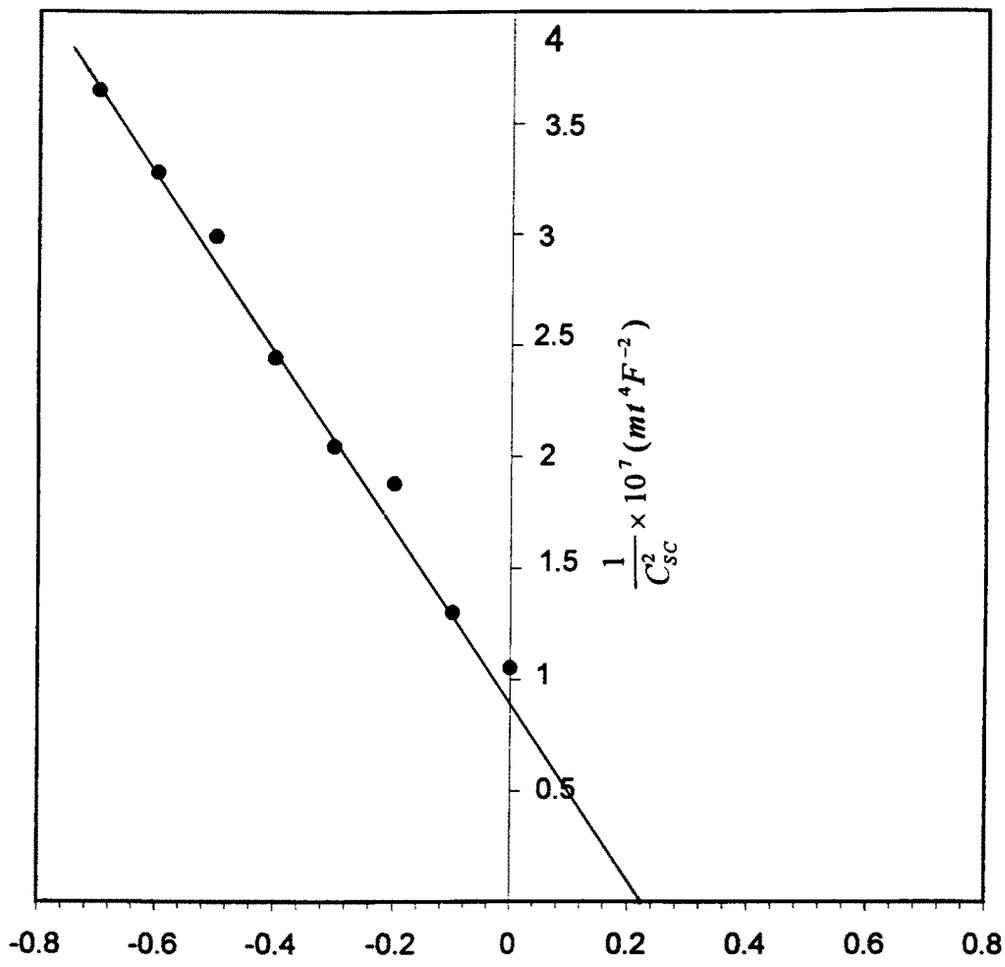

Fig. 9.4 Mott Schottky plot for p-WSe_2 single crystal.

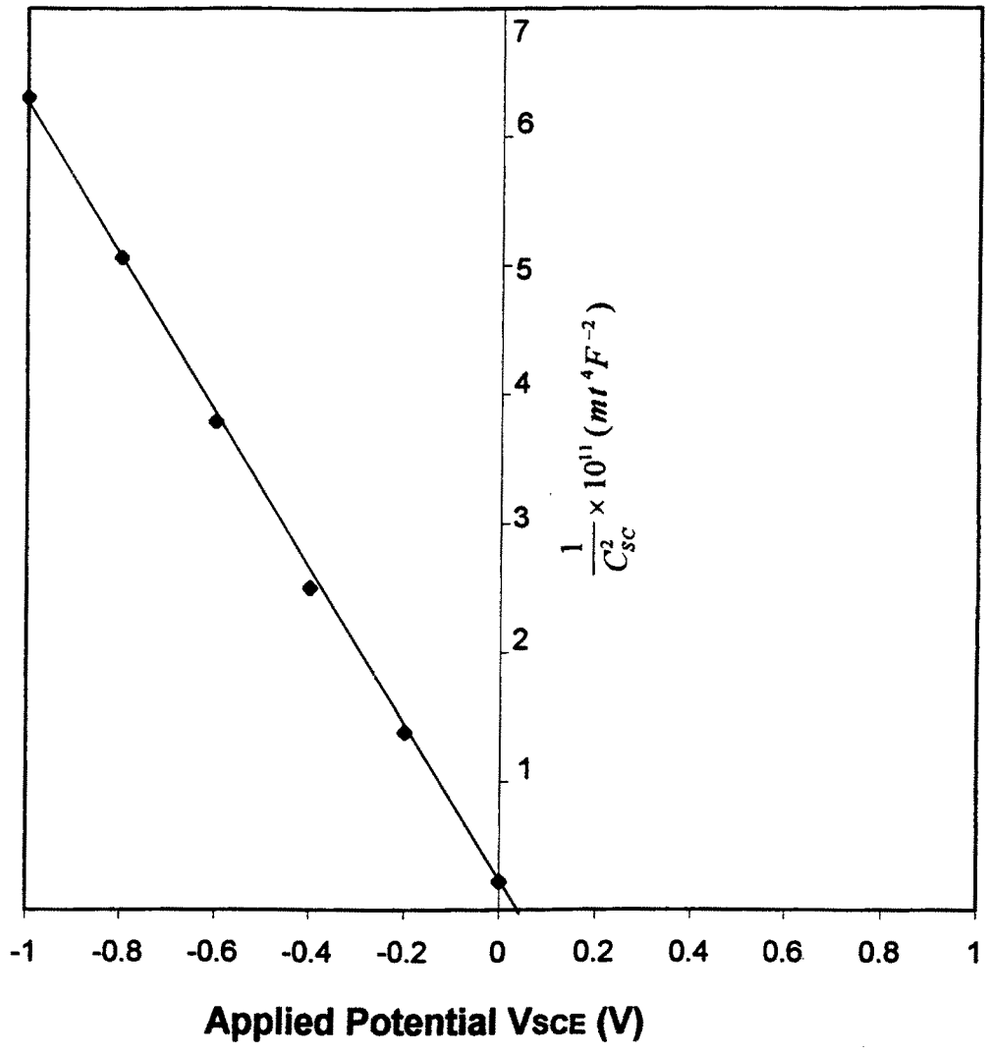

Fig. 9.5 Mott Schottky plot for WSSe single crystal.

Table 9.4 : Summary of the Results Obtained from the Mott - Schottky Plots of WSe_2 and WSSe Single Crystals.

Properties	WSe_2	WSSe
Type	p	p
Band gap (E_g) (eV)	1.44	1.65
Electrolyte used	0.025M I_2 + 1M NaI + 2M Na_2SO_4 + 0.5M H_2SO_4	
Flat band potential V_{fb} (eV)	0.22	0.04
Band bending V_b (eV)	0.59	0.41
Acceptor concentration (m^{-3})	$N_A = 1.96 \times 10^{21}$	$N_A = 2.005 \times 10^{17}$
Density of states in the valence band (m^{-3})	$N_V = 9.80 \times 10^{28}$	$N_V = 1.085 \times 10^{28}$
Depletion width W (m)	7.74×10^{-7}	5.1×10^{-5}
Conduction band edge E_c (eV)	0.678 eV	0.735 eV
Valence band edge E_V (eV)	- 0.762	- 0.915
Redox fermi level of electrolyte $E_{F,redox}$	0.370	0.370

The dielectric constant ε for WSe_2 and WSSe crystals has been evaluated by using the relation

$$\varepsilon = \frac{Cd}{A\varepsilon_0} \tag{9.2}$$

Where C is the capacitance, d is the thickness of the crystal, and A is the area of contact. The values of ε using this formula for WSe_2 and WSSe are obtained as 18 and 11.5 respectively.

Upon inserting the values of all the parameters in equation (9.1) the acceptor concentration N_A (Table 9.4) for WSe_2 and WSSe are obtained as 1.96×10^{21} and 2.005×10^{17} m^{-3} respectively.

9.2.6.3 Energetic band location :

From the values of the bandgaps for WSe_2 and WSSe, the positions of the valence band and conduction band edges for both the electrodes in the electrolyte reported above can be estimated. The procedure for this estimation is outlined below :

For WSe_2 and WSSe, which are p-type, the difference between E_V and E_f can be obtained from the equation

$$N_A = N_v \exp (E_v - E_F)/kT \tag{9.3}$$

Where N_A is the acceptor density (all acceptor impurities assumed to be completely ionised), E_v is the energy at the edge of the valence band; E_F is the fermi level energy and N_v the density of effective states in

the valence band, which is given by

$$N_v = \frac{2}{h^3}\left(2\pi m_e^* kT\right)^{\frac{3}{2}} \tag{9.4}$$

For determination of effective mass m_e^* in this formula, we use the expression (Chapter 5).

$$\left(m_h^*\right)^{\frac{3}{2}} = \frac{1}{2\left(2\pi kT\right)^{\frac{3}{2}}} \ln^{-1}\left[\frac{Se}{k} - 2 + \ln\left(ph^3\right)\right] \tag{9.5}$$

The values of Seebeck coefficient S and carrier concentration p for WSe_2 and WSSe at room temperature were obtained in the manner outlined in Chapter 2 and are listed in Table 9.5. The values of resistivity as determined using van der Pauw method for both these crystals are also given in this table. Putting these values of S and p in equation 9.5, values of effective mass m_e^* have been obtained at room temperature (300 K) for WSe_2 and WSSe and are given in Table 9.5. Taking these values of effective mass, the values of N_V (Table 9.4) have been estimated for WSe_2 and WSSe as 9.80×10^{28} and 1.085×10^{28} m^{-3} respectively.

From equation 9.3, we can write

$$\ln N_A = \ln N_V + (E_V - E_F)/kT$$

$$\text{or} \quad E_F - E_V = kT \ln \left(\frac{N_V}{N_A}\right) \tag{9.6}$$

Using this relation, $E_F - E_V$ has been evaluated for WSe_2 and WSSe and the values are shown in Table 9.4. From the values of V_{fb}, the

Table 9.5 : Resistivity (ρ), Carrier Concentration 'p', Seebeck coefficient (S) and effective mass (m_e^*) for WS_2 and WSSe single crystals at room temperature.

Material	Resistivity 'ρ' Ω cm	Carrier Concentration 'p' m^{-3}	Seebeck Coefficient 'S' $\mu V K^{-1}$	Effective mass m_h^* Kg
WSe_2	0.185	1.45×10^{23}	1326×10^{-6}	2.262×10^{-28}
WSSe	1.018	4.34×10^{22}	1240×10^{-6}	5.21×10^{-29}

values of E_V for both the compounds have been estimated and are represented in Table 9.4. Now taking the values of energy band gap E_g for WSe_2 as 1.44 eV and for WSSe as 1.65 eV, the position of conduction band minimum for both the materials have been obtained and are given in Table 9.4. The complete energy level diagrams for the PEC cells fabricated with WSe_2 and WSSe in the electrolyte (0.025M I_2 + 1M NaI + 2M Na_2SO_4 + 0.5M H_2SO_4) have been prepared and are shown in Fig. 9.6.

The band bending, V_b is an important parameter, since it gives the maximum open circuit voltage obtainable from a photoelectrochemical cell. V_b and V_{fb} are related as

$$V_b = V_{f,\,redox} - V_{fb} \qquad (9.7)$$

The values of V_b for both the electrodes of WSe_2 and WSSe have been determined using this relation and are listed in Table 9.4.

Further, substituting the values of N_A and V_b from Table 9.4 into the equation

$$W = (2\,\varepsilon\,\varepsilon_o\,V_b/e\,N_A)^{1/2} \qquad (9.8)$$

The width of the space charge region W has been evaluated for the representative electrodes in the given electrolyte. These values are also shown in Table 9.4.

The value of $V_{f,redox}$ in this table have been measured using a pH meter with a SCE electrode.

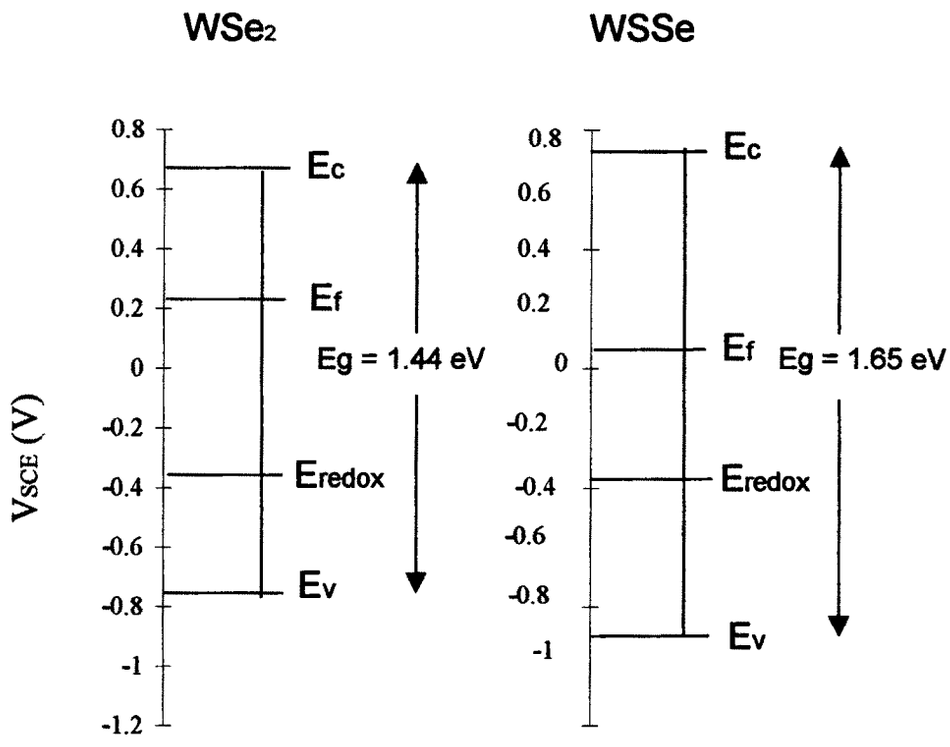

Fig 9.6 Energy band diagrams for WSe_2 and WSSe single crystals in the electrolyte.

9.2.7 EFFECT OF SUBSTITUTION OF SELENIUM BY SULPHUR ON THE PHOTORESPONSE OF WSe_2 :

In order to see the effect of substitution of selenium by sulphur in WSe_2 the surfaces of both the electrodes i.e. WSe_2 and WSSe were taken after cleaving them with an adhesive tape. Since the photoresponse of an electrode depends upon its surface area and the surface areas of the electrodes of WSe_2 and WSSe are not same, a quantity representing photoresponse per unit area should be evaluated for both the electrodes. In order to watch the effect of substitution of selenium by sulphur on WSe_2, current density (J) vs voltage characteristics for electrodes of WSe_2 and WSSe were drawn as shown in Figs. 9.7 and 9.8. The data for these plots are given in Tables 9.6 and 9.7. The solar cell parameter e.g. I_{sc}, V_{oc}, the maximum power (P_{max}), the voltage at maximum power (V_{max}), the fill factor (FF) and the efficiency (η) were determined from these plots are given in Tables 9.6 and 9.7 for WSe_2 and WSSe crystals respectively.

9.3 DISCUSSION :

The nature of Mott-Schottky plots firmly confirm the p-type behaviour of the single crystals of WSe_2 and WSSe used in the present study. The photoresponse studies carried out in electrolytes of different compositions established that the electrolyte with the composition "0.025M I_2 + 1M NaI + 2M Na_2SO_4 + 0.5M H_2SO_4" is the most suitable and befitting electrolyte for the present work. The energetic location of the valence and conduction bands carried out above also confirms the suitability of the above electrolyte for both the electrodes, since the redox potential of this electrolyte lies within the bandgap.

The data presented in Tables 9.6 and 9.7 obviously indicate that

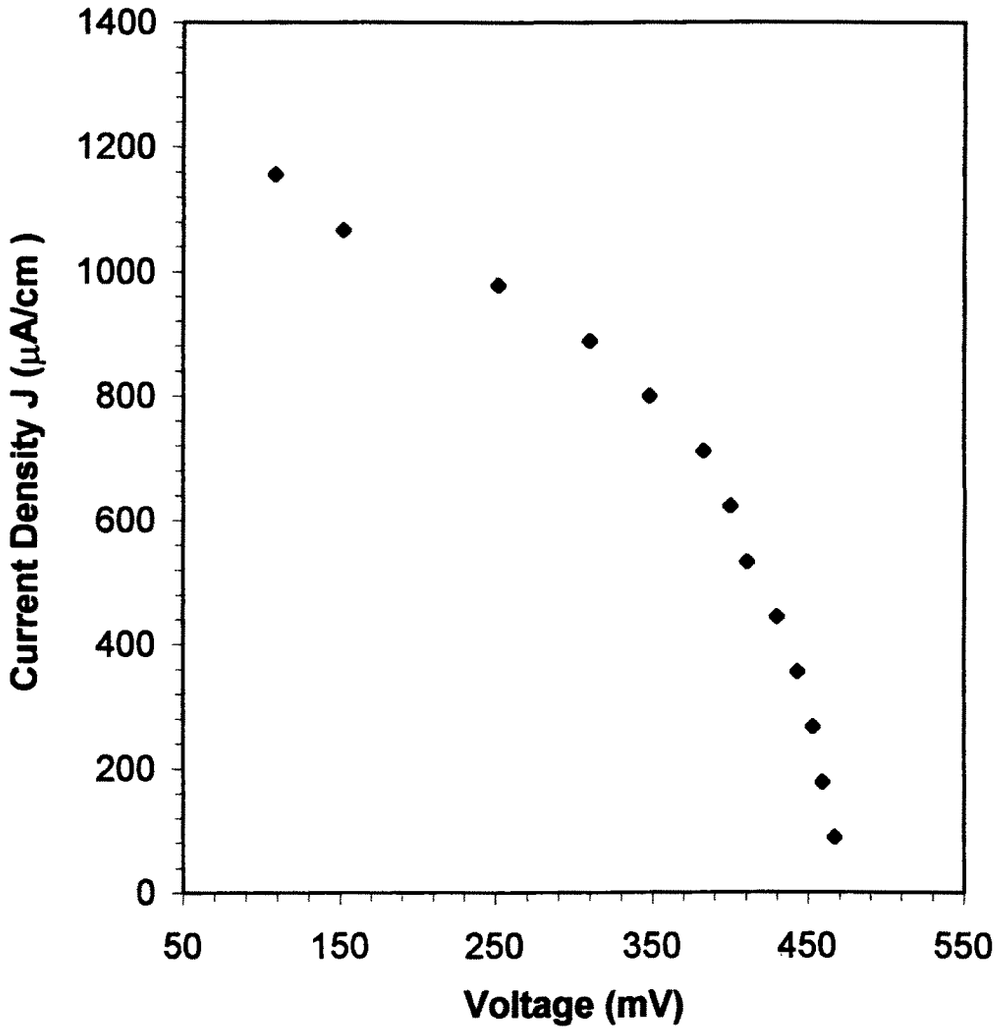

Fig. 9.7 J - V Characteristics for WSe_2 electrode

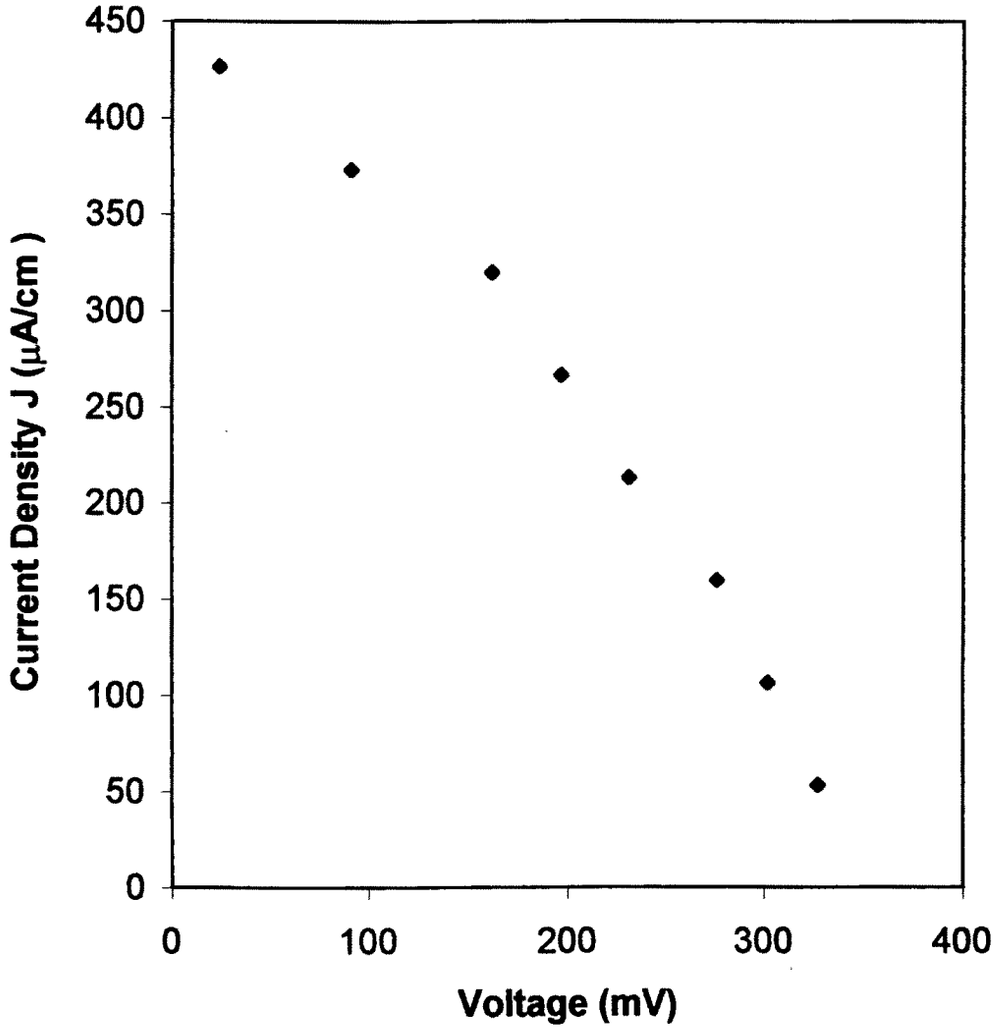

Fig. 9.8 J - V Characteristics for WSSe electrode

Table 9.6 : Photoresponse of WSe_2 single crystals as photoelectrode

Electrolyte : 0.025M I_2 + 1M NaI + 2M Na_2SO_4 + 0.5M H_2SO_4

Intensity : 100 mWatt / cm^2

I_{sc} : 120 μA I_D : 0.1 μA

V_{oc} : 470 mV V_D : 0.1 mV

P_{max} : 31320 $\times 10^{-9}$ Watt

V_{max} : 348 mV

f. f. : 0.56

η (%) : 0.28 %

Area exposed : 0.1125 cm^2

Current Density (J) ($\mu A/cm^2$)	Voltage (mV)
088.8	467
177.7	459
266.6	453
355.5	443
444.4	430
533.3	411
622.2	400
711.1	383
800.0	348
888.8	310
977.7	252
1066.6	152
1155.5	109

Table 9.7 : Photoresponse of WSSe single crystals as photoelectrode

Electrolyte : 0.025M I_2 + 1M NaI + 2M Na_2SO_4 + 0.5M H_2SO_4

Intensity : 100 mWatt / cm^2

I_{sc} : 16.5 μA I_D : 0.1 μA

V_{oc} : 350 mV V_D : 0.1 mV

P_{max} : 1970 $\times 10^{-9}$ Watt

V_{max} : 197 mV

f. f. : 0.34

η (%) : 0.05 %

Area exposed : 0.0375 cm^2

Current Density (J) ($\mu A/cm^2$)	Voltage (mV)
53.3	327
106.6	302
160.0	276
213.3	231
266.6	197
320.0	162
373.3	91
426.6	24

(i) The photoelectrochemical properties of WSSe are inferior to those of WSe_2 single crystals

(ii) The conversion efficiency, η, of WSe_2 phase is 0.28% and in fact higher than that of WSSe.

It is seen from the data presented in Table 9.5 that the effect of partial replacement of selenium by sulphur in WSe_2 is to make the material more resistive. This is probably the reason for higher efficiency in WSe_2 as compared to WSSe. Hence the increased efficiency in WSe_2 can be attributed to the lower bulk resistivity of this material as compared to WSSe, which is prepared by the partial replacement of selenium, by sulphur in WSe_2

The values of efficiencies so obtained in the present work with WSe_2 and WSSe are too low for any practical utility. Since the aim of the present work was to notice the effect of partial replacement of selenium by sulphur in the lattice of WSe_2 on the photoresponse of WSe_2, not with a standing efforts to improve the efficiencies of the solar cells were considered here.

Although metal dichalcogenide semiconductors are amongst the most studied semiconductors for PEC solar cell, one of the major shortcomings of this class of materials is that steps and dislocations on the van der Waals (vdW) face serve as the recombination centres thus limiting the collection (quantum) efficiency of the cell. Conversion efficiencies in excess of 10% can be achieved only after a careful cleavage of vdW face of the crystal [6] and after an annealing treatment to the photoelectrode surface, it was ensured that proper ohmicity of the contacts could be obtained with the crystals. Srivastava and Pathak [17] in their studies expressed that the processing of the back contact with the

electrodes by giving a heat treatment at 200° C for 24 hours significantly improves the photoresponse of the $MoSe_2$ electrodes.

Furthermore, higher values of efficiencies can be obtained only with crystals having ideally smooth surfaces. Even, seemingly smooth surfaces exhibit very fine steps when examined in interference contrast optical microscope [18]. Therefore one has to ascertain the smoothness of the samples very carefully before it is used for the fabrication of a PEC solar cell with extremely higher values for the photoconversion efficiency.

If one is unable to get an ideally smooth surface then ways to passivate the recombination centres on the surface of a layered semiconductor shall have to be discovered. An approach to such an effort was made by Simon et al [19] who collected the traces of microscopic metal islands deposited electrochemically on the surface of MS_2 (M = Mo, W) leading to a large improvement in the charge transfer kinetics across the semiconductor/electrolyte interface. More efforts for passivation have been urged by several other investigators [18, 20-23].

In years to come, photoelectrochemical etching (Photoetching) was extensively used for the preferential etching of defects and recombination centres from the surface of various semiconductors [24,25]. Convincingly appreciable improvements in the PEC's constructed from these materials have been thoroughly come into force now [26].

9.4 CONCLUSIONS :

Conclusively, author admits that normally grown surfaces of layered materials permit very low values of photoconversion efficiencies

[27,28] but concentrated efforts are to be made in selection of a suitable material with the result that effective efficiency improvements can be achieved by

1. Reducing the reflectivity of the semiconductor electrode surface,

2. Decreasing the surface and bulk recombination rate,

3. Lowering the bulk resistivity of the material, and

4. Minimising the absorption losses in the electrolyte.

Partial replacement of selenium by sulphur in WSe_2 does not yield any improvement in its PEC behaviour. Nevertheless, overall efficiencies of the cells can be increased only through the methods discussed in the above para.

REFERENCES :

1. Photoelectrochemistry and Photovoltaics of layered semiconductors
   Ed. A. Aruchamy, Kluwer Academic Publishers, Dordrecht (1992)

2. B. Fotouhi and A. Katty,
   Electrochimica Acta, **31** (1986) 795

3. B. Fotouhi and A. Katty,
   Electrochimica Acta, **32** (1987) 1149

4. A. Katty, B. Fotouhi and O. Gorochov,
   J. Electrochem. Soc., **131** (1984) 2806

5. F.R. Fan, H.S. White, B. Wheeler and A.J. Bard,
   J. Electrochem. Soc., **127** (1980) 518

6. R. Tenne and A. Wold,
   Appl. Phys. Lett., **47** (1985) 707

7. G.Prasad and O.N. Srivastava,
   J.Phys. (D) (Appl. Phys.), **21** (1988) 1028

8. G. Campet, C. Azaiez, F. Levy, H. Bourezc and J. Claverie,
   Active and Passive Elec. Comp., **13** (1988) 33

9. J. Gobrecht, H. Tributsch and H. Gerischer,
   J. Electrochem. Soc., **125** (1978) 2085

10. D. Canfield and B.A. Parkinson,
    J. Am. Chem. Soc., **103** (1981) 1279

11. K.K. Kam and B.A. Parkinson,
    J. Phys. Chem., **86** (1982) 463

12. G. Prasad, N.N. Rao and O.N. Srivastava
    Int. J. Hydrogen Energy, **13** (7) (1988) 399

13. Amita Chandra, R.N. Pandey, O.N. Srivastava and G.Prasad,
    Semicond. Sci. Technol., **6** (1991) 137

14. G.Prasad and O.N. Srivastava
    Semicond. Sci. Technol., **8** (1993) 2161

15. G. Hodes, E. Watkins, D. Mantell, L.J. Brillson,M. Peisach and A. Wold
J. Appl. Phys., **71** (10) (1992) 5077

16. R. Bourezg, G. Couturier, J. Salardenne, J.P. Doumerc and F. Levy,
Phys. Rev. B., **46** (23) (1992) 15411

17. R.Srivastava and V.M. Pathak,
J. Mater. Sci. Lett., **9** (1990) 294

18. D. Mahalu, L. Margulis, A. Wold and R. Tenne,
Phys. Rev. B., **45** (4) (1992) 1943

19. R.A. Simon, A.J. Ricco, D.J. Harrison and M.S.Wright,
J. Phys. Chem., **87** (1983) 4446

20. L. Fornarini, F. Stirpe and B. Scrosati,
J. Electrochem. Soc., **130** (1983) 2184

21. L.Fornarini and B. Scrosati,
Electrochim. Acta, **28** (1983) 667

22. C. Levy Clement, S. Arvamuthan and K.S.V. Santhanam,
J. Electroanal. Chem., **248** (1988) 233

23. S.Arvamuthan, C. Levy Clement, S. Madhavan and K.S.V.Santhanam,
J. Power Sources, **32** (1990) 1

24. G. Hodes, D. Cahen and H. Leamy,
J. Appl. Phys., **54** (1983) 4676

25. M. Tomkiewicz, W. Siripale and R. Tenne,
J. Electrochem. Soc., **131** (1984) 736

26. R. Tenne and G. Hodes,
Appl. Phys. Lett., **37** (1980) 428

27. H.S. White, H.D. Abruna and A.J. Bard,
J. Electrochem. Soc., **129** (1980) 266

28. W. Kautek, J. Gobrecht and H. Gerischer,
Ber. Bunsenges Phys. Chem., **84** (1980) 1034.